Analysis of Lightning-Radiated Electromagnetic Fields in the Vicinity of Lossy Ground

Abdolhamid Shoory, Rouzbeh Moini, *Member, IEEE*, S. H. Hesam Sadeghi, *Member, IEEE*, and Vladimir A. Rakov, *Fellow, IEEE*

***Abstract*—An antenna theory (AT) approach in the frequency domain is presented to compute electromagnetic fields radiated by a lightning return stroke. The lightning channel is modeled as a lossy-wire monopole antenna (a wire antenna with distributed resistance) energized by a current source at its base, and the ground is modeled as a lossy half-space. The method of moments is used for solving the governing electric field integral equation (EFIE) in the frequency domain. The resultant current distribution along the channel is used to calculate electromagnetic fields at different distances from the channel. All field components are evaluated using a rapid but accurate procedure based on a new approximation of Sommerfeld integrals. In contrast with the previous models, the approach proposed here is characterized by a self-consistent treatment of different field components in air or on the surface of a lossy half-space. It is shown that the omission of surface wave terms in the general field equations, as done in the perfect-ground approximation, can strongly affect model-predicted field components.**

***Index Terms*—Electromagnetic fields, lightning return stroke, lossy ground, method of moments (MoM).**

I. Introduction

INTERACTION of lightning-radiated electromagnetic fields with electric power lines and other electrical circuits can cause malfunction or even destruction of critical installations. In order to design an adequate lightning protection system, a detailed understanding of lightning and its electromagnetic fields is necessary. Many models have been proposed to describe the behavior of lightning and predict its effects. All of these models can be placed in four categories [1], namely physical models, distributed-circuit models, engineering models, and electromagnetic models. The last two categories of models can be conveniently tested against observations.

Engineering models specify a closed-form relation between the current distribution along the channel and current at the channel base. The most used engineering models can themselves be classified into two categories. The first category includes traveling-current-source-type models. The Diendorfer–Uman (DU) model and the traveling current source (TCS) model are placed in this category. The second category contains transmission-line-type models, namely the transmission-line (TL) model, the modified transmission-line model with linear current decay with height (MTLL), and the modified transmission-line model with exponential current decay with height (MTLE). Electromagnetic models, on the other hand, are usually based on antenna theory and thin-wire approximation for the lightning channel. In these models, Maxwell's equations are solved numerically to obtain a current distribution along the channel, using which remote electromagnetic fields are readily computed. An overview and comparison of recently published models are found in the works of Rakov and Uman [1], Nucci *et al.* [2], Thottappillil and Uman [3], Thottappillil *et al.* [4], and Rakov [5], [6].

A great deal of attention has been recently devoted to the electromagnetic models [or alternatively antenna theory (AT) models] [5], [7]–[18]. In these models, the lightning return stroke channel is usually considered as a monopole wire antenna above a perfectly conducting ground. The governing electric field integral equation (EFIE) is solved for the distribution of current along the channel in either the time or frequency domain.

Moini *et al.* [7] solve the EFIE in the time domain. In finding the current distribution, propagation velocities lower than light velocity are achieved assuming that the antenna is surrounded by a dielectric medium with permittivity greater than that of free space (once the current distribution is known, the antenna is allowed to radiate in free space). Also, attenuation of the upward traveling current wave is accounted for using distributed resistance along the channel. The resultant current distribution is employed to calculate free space electromagnetic fields. It is worth mentioning that due to radiation losses, the current suffers attenuation and dispersion as it propagates along the channel, even when the channel is modeled as a perfectly conducting wire [9], [13]. The method requires suitable adjustment of sampling rate and wire segmentation to avoid undesirable divergence of numerical results. Ishii and Baba [8], [14] make use of the numerical electromagnetic code (NEC-2) [19] and solve the EFIE in the frequency domain. They achieve the attenuation of the upward traveling current wave and realistic propagation velocities by introducing appropriate distributed resistance and inductance, respectively. As with other frequency-domain analysis methods of transient phenomena, it is necessary to appropriately adjust sampling rate and total analysis time to avoid undesirable aliasing or circular convolution. Both methods make use of a voltage source at the channel base whose waveform is tuned to generate the desired current at the lightning channel base. Shoory *et al.* [15], Grcev *et al.* [16], and Baba and Rakov

Manuscript received September 29, 2003; revised May 17, 2004. This work was supported in part by the Tehran Regional Electric Company under Grant 10-78/10/15 and in part by the National Science Foundation under Grant ATM-0003994.

A. Shoory, R. Moini, and S. H. H. Sadeghi are with the Electrical Engineering Department, Amirkabir University of Technology, Tehran 15914, Iran (e-mail: moini@aut.ac.ir).

V. A. Rakov is with the Electrical and Computer Engineering Department, University of Florida, Gainesville, FL 32611 USA (e-mail: rakov@ece.ufl.edu).

Digital Object Identifier 10.1109/TEMC.2004.842104

[17] used current sources in their electromagnetic models of lightning return stroke.

Further, considerable efforts have been dedicated to examine field components when the ground has finite conductivity, and several exact and approximate solutions have been proposed. The so-called wavetilt formula relates the Fourier transform of the horizontal electric field to that of the vertical one by a frequency-dependent multiplication factor [20]. The formula is appropriate for remote observation points and is not applicable to close ranges. This method was widely used by several authors (e.g., [21]) to calculate induced voltages on overhead power lines. Using the ground's surface impedance, Cooray [22] calculated the horizontal electric field at the ground surface from the horizontal magnetic field. He has shown that this approximate method produces accurate results for ranges as close as 200 m. Rubinstein [23] introduced a new formula, presently referred to as the Cooray–Rubinstein formula, in which the horizontal electric field at a specified height is composed of two terms. One is the horizontal electric field calculated at a given height using the perfect-ground assumption, and the other is the horizontal magnetic field at ground level, again calculated using the perfect-ground assumption, multiplied by the ground's surface impedance. It is shown that this latter approach is more reasonable than the two former ones [24]. Some generalizations and modifications to the Cooray–Rubinstein formula have been proposed. Wait [25] developed an exact version of this formula in the frequency domain and identified the conditions under which it reduces to the Cooray–Rubinstein formula. Cooray [26] presented a detailed examination of the problem. He has shown that the horizontal electric field at ground level can be calculated accurately using the Cooray–Rubinstein formula, even for very close observation points. However, the horizontal electric field above ground deviates by more than 25% from its exact value, depending on the ground conductivity and height of the observation point. He proposed a simple modification to the Cooray–Rubinstein formula that reduced its error to less than 5%. In the following, we refer to this modification as the Cooray modified formula.

Distortion of the vertical electric field due to ground's finite conductivity has also attracted considerable attention. A discussion of this issue is found, for example, in the works of Cooray and Lundquist [27] and Fernando and Cooray [28]. Using an approach proposed by Wait [29], Cooray and Lundquist [27] calculated the electric field over an imperfectly conducting ground from its counterpart over a perfect ground. It was shown that the propagation effects could change the peak and rise time of a radiated electric field. Propagation effects include the preferential attenuation of the higher frequency components in the vertical electric and azimuthal magnetic fields.

Further, communication lines are often laid underground. Despite the common belief that these installations are less susceptible to effects of lightning electromagnetic fields than overhead ones, their relatively low withstand levels to external overvoltages make them vulnerable to such effects. Cooray [30] proposed a time-domain solution for underground electromagnetic fields and related these fields to their surface counterparts.

The lightning channel above lossy half-space represents the so-called generalized Sommerfeld half-space problem [25], [26]. This problem was formulated by Sommerfeld and later examined by several other researchers. In [31], the effects of two media interface on the radiated electromagnetic fields of a dipole have been completely formulated and accurately analyzed from both the mathematical and physical points of view. Banos [32], using the solution of Maxwell's equations in each medium and applying boundary conditions at the interface, found a complete explanation of the problem. The resulting equations are based on semi-infinite integrals of Bessel functions, referred to as Sommerfeld integrals. These integrals are highly oscillatory and weakly damping, and there exists no closed-form solution for their evaluation. Considerable work has been done to evaluate these integrals numerically [33], [34] or at least to obtain closed-form approximations in some special cases [35], [36]. A suitable solution needs to minimize the number of these integrals and to efficiently evaluate them for arbitrary orientation of the dipole and over a wide frequency range. Some recent solutions [37]–[39] satisfy the necessary requirements.

In this paper, we propose a new AT model of lightning return stroke above a lossy half-space in the frequency domain. The half-space problem is solved using a nearly exact approximation to Sommerfeld integrals. The return stroke channel is considered as a lossy-wire monopole antenna [7] with a current source at its input terminals as opposed to the voltage source used in most of the previously published electromagnetic models (e.g., [7] and [14]). The use of a current source is more realistic and convenient than the use of a voltage source. This approach eliminates the preliminary steps that include the determination of antenna input impedance. Distributed resistance is used to include attenuation of the upward traveling current wave. Propagation velocities lower than light velocity are achieved in finding the current distribution by letting the antenna radiate in a medium with permittivity greater than that of free space [7]. Once the current distribution is known, remote field calculations are performed in the free half-space. Lossy ground is included in two different ways. First, in evaluating the current distribution along the channel, we use the modified image theory approach proposed by Takashima *et al.* [40] and utilized in some studies of grounding systems [41], [42]. In this case, due to the near-zone observation points (placed on the wire surface), contributions from surface waves are reasonably neglected. Second, in evaluating remote field components, we employ the complete, nearly exact expressions for lightning electromagnetic fields over lossy ground (land or sea). This is a generalization to the methodology described in [43]. It will be shown later that the expressions for fields of a vertical dipole each contain a term related to the direct wave from the dipole, a term related to the reflected wave from its perfect image, and a term, including Fresnel integrals, related to the surface wave (lateral wave).

To derive the above-mentioned field expressions, the Sommerfeld problem is revisited. Subject only to one condition, which is acceptable in the present problem, a nearly exact approximation to Sommerfeld integrals is applied and closed-form expressions are obtained. In spite of its simplicity, the methodology is not only accurate but also efficient in terms of computer memory and time. This technique, in contrast with those found in previous publications, provides a self-consistent

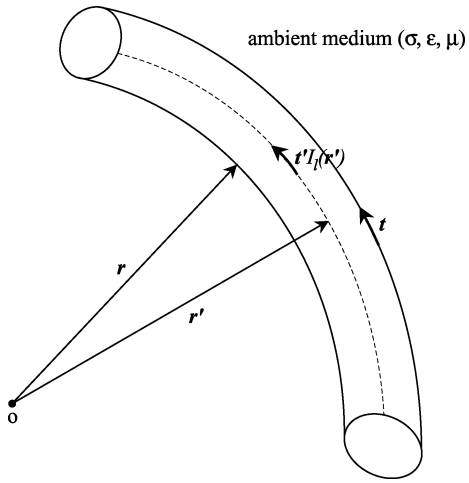

Fig. 1. Thin-wire approximation.

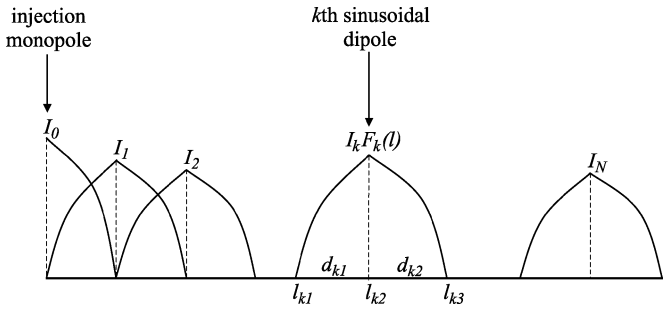

Fig. 2. Sinusoidal current expansion.

treatment for all field components. It is also shown that the Cooray–Rubinstein formula is an approximation to the more general formula for the horizontal electric field employed here, although the derivation approaches are quite different.

The paper is organized as follows. In Section II, the problem is formulated in the frequency domain. The Galerkin method is used to solve the governing EFIE addressing the challenges related to the use of current source in the proposed AT model. The effects of lossy ground are included in both evaluating the current distribution along the channel and computing remote electromagnetic field components. In Section III, current distributions and associated remote field components for the case of a perfect ground are computed using the proposed approach and compared with those obtained using the AT model described in [7]. Also, a comparison is made between the Cooray–Rubinstein formula (and the Cooray modified formula [26]) for the horizontal electric field and the generalized expression for the horizontal electric field employed in this paper. Finally, various field components over different lossy media are computed and discussed.

II. Theory

A. Frequency-Domain Analysis

In the analysis of lightning electromagnetic fields, the current waveform at the lightning channel base is given in the time domain, and electromagnetic field quantities are usually required to be in the time domain. Since the method presented in this paper adopts a frequency-domain approach, an appropriate fast Fourier transform (FFT) algorithm is used for spectral representation of the lightning channel-base current. Conversion back to the time domain is achieved by applying an inverse FFT (IFFT) technique to the derived frequency spectra of required quantities. It is worth mentioning that, throughout this paper, the time dependence of $e^{j\omega t}$ is suppressed for convenience.

B. Electric Field Integral Equation (EFIE)

Consider a perfectly conducting wire placed in a medium with conductivity σ, permittivity ε, and permeability μ, shown in Fig. 1. The EFIE expresses the fact that the total tangential electric field on the wire surface vanishes

$$\boldsymbol{t}\cdot(\boldsymbol{E}^i+\boldsymbol{E}^s)=0 \tag{1}$$

where $\boldsymbol{t}$ denotes a unit vector tangential to the wire surface, and the two terms in the parentheses are the incident ($\boldsymbol{E^i}$) and scattered ($\boldsymbol{E^s}$) fields. The wire antenna representing a lightning channel satisfies the thin-wire approximation [44] since its radius is much smaller than the smallest wavelength, and its length is much greater than the radius. This implies that: 1) current on the wire flows only in the longitudinal direction and 2) circumferential or radial variations in the axial current are negligible. Consequently, the longitudinal current can be considered as a filamentary line on the wire axis (see Fig. 1) that produces the scattered field given by

$$\boldsymbol{E}^s(\boldsymbol{r})=\frac{1}{4\pi(\sigma+j\omega\varepsilon)}\int_l\{[\boldsymbol{t'}I_l(\boldsymbol{r'})\cdot\nabla]\nabla g(\boldsymbol{r},\boldsymbol{r'})-\gamma^2\boldsymbol{t'}I_l(\boldsymbol{r'})g(\boldsymbol{r},\boldsymbol{r'})\}\,dl \tag{2}$$

where $\boldsymbol{t'}$ is the unit vector along wire axis, $I_l(\boldsymbol{r'})$ is the longitudinal current to be determined, and $\boldsymbol{r}$ and $\boldsymbol{r'}$ are vectors denoting the observation and source points, respectively. Also, $\gamma(=\sqrt{j\omega\mu(\sigma+j\omega\varepsilon)})$ is the medium complex wave number, and $g(\boldsymbol{r},\boldsymbol{r'})(=e^{-\gamma R}/R)$ is the homogeneous medium Green's function, where $R=|\boldsymbol{r}-\boldsymbol{r'}|$. Combining (1) and (2) yields the governing integral equation from which the longitudinal current can be found.

C. Method of Moments and Concept of Current Source

To solve the governing EFIE for longitudinal current distribution on the wire ($I_l(l)$, it is expanded in a finite series of N overlapped sinusoidal dipoles and an additional sinusoidal monopole at the current injection point, as depicted in Fig. 2:

$$I_l(l)=\sum_{k=0}^{N}I_kF_k(l) \tag{3}$$

where I_k are the unknowns to be determined, l is the distance along the wire, and $F_k(l)$ are the normalized sinusoidal currents

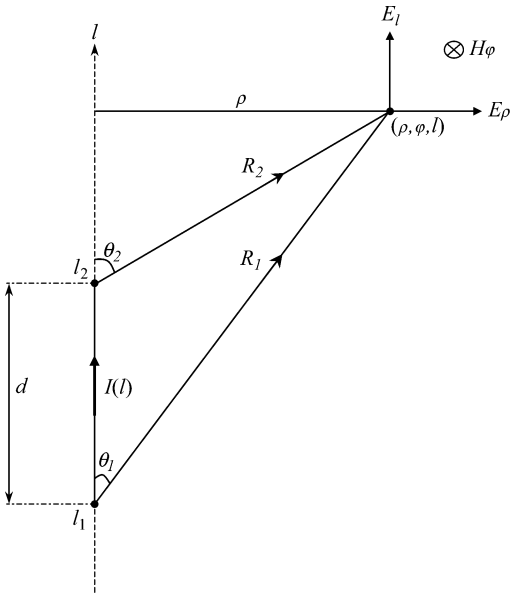

Fig. 3. Geometry of sinusoidal monopole and its electromagnetic fields.

over the length of one dipole or injection monopole, expressed as follows [44]:

$$F_k(l) = \frac{P_{k1}(l)\sinh\gamma(l-l_{k1})}{\sinh\gamma d_{k1}} + \frac{P_{k2}(l)\sinh\gamma(l_{k3}-l)}{\sinh\gamma d_{k2}}$$
$$P_{k1}(l) = \begin{cases} 1, & l_{k1} \le l \le l_{k2} \\ 0, & \text{elsewhere} \end{cases}$$
$$P_{k2}(l) = \begin{cases} 1, & l_{k2} \le l \le l_{k3} \\ 0, & \text{elsewhere} \end{cases} \tag{4}$$

where, for the kth dipole, l_{k2} is the mid (terminal) point, l_{k1} and l_{k3} are the end points ($k = 1, 2 \ldots N$), and d_{k1} and d_{k2} are the dipole-arm lengths. For the injection monopole ($k = 0$), only the second term of (4) is used.

Applying (3) and (4) to (1) and (2) and using the Galerkin method, one can obtain a system of N linear algebraic equations of the form $\boldsymbol{ZI} = \boldsymbol{V}$, where $\boldsymbol{I}$ is the current vector to be solved for, $\boldsymbol{V}$ is the excitation vector, and $\boldsymbol{Z}$ is the impedance matrix. Evaluating the elements of $\boldsymbol{Z}$ and $\boldsymbol{V}$ requires numerical double integrations. To increase computation efficiency and accuracy, it is desirable, when possible, to replace numerical integrations with appropriate analytic expressions. Such an alternative exists only for the sinusoidal current expansion [44] whose near-field expressions are available in rigorous form. Rigorous field expressions of a sinusoidal monopole in cylindrical coordinate system (see Fig. 3) are given as follows [45], [46]:

$$E_\rho = \frac{\gamma}{\rho(\sigma+j\omega\varepsilon)}\frac{1}{4\pi\sinh\gamma d} \times \left[(I_1 e^{-\gamma R_1} - I_2 e^{-\gamma R_2})\sinh\gamma d + (I_1\cosh\gamma d - I_2)e^{-\gamma R_1}\cos\theta_1 + (I_2\cosh\gamma d - I_1)e^{-\gamma R_2}\cos\theta_2\right] \tag{5}$$

$$E_l = \frac{\gamma}{(\sigma+j\omega\varepsilon)}\frac{1}{4\pi\sinh\gamma d} \times \left[(I_1 - I_2\cosh\gamma d)\frac{e^{-\gamma R_2}}{R_2} + (I_2 - I_1\cosh\gamma d)\frac{e^{-\gamma R_1}}{R_1}\right] \tag{6}$$

$$H_\varphi = \frac{1}{4\pi\rho\sinh\gamma d} \times \left[(I_1\sinh\gamma d\cos\theta_1 + I_1\cosh\gamma d - I_2)e^{-\gamma R_1} - (I_2\sinh\gamma d\cos\theta_2 - I_2\cosh\gamma d + I_1)e^{-\gamma R_2}\right] \tag{7}$$

where I_1 and I_2 are the values of monopole current, $I(l)$, at l_1 and l_2, respectively:

$$I(l) = \frac{I_1\sinh\gamma(l_2-l) + I_2\sinh\gamma(l-l_1)}{\sinh\gamma d}. \tag{8}$$

Other quantities are depicted in Fig. 3. Using these field components, one can replace the inner integrals for $\boldsymbol{Z}$ and $\boldsymbol{V}$ by their analytic expressions.

To show the advantages of the current–source excitation, we first consider the voltage source case. In this latter case [7], [8], [13], [14], the source voltage $V(f)$ is obtained as follows:

$$V(f) = Z_{\text{in}}(f)\cdot I(f) \tag{9}$$

where $Z_{\text{in}}(f)$ is the input impedance of the wire antenna, and $I(f)$ is the Fourier transform of the specified channel-base current. Once the exciting voltage is obtained, it can be used in the following $(N+1)\times(N+1)$ linear matrix equation to obtain the current distribution:

$$\begin{pmatrix} z_{00} & z_{01} & \cdots & z_{0N} \\ z_{10} & z_{11} & \cdots & z_{1N} \\ \vdots & \vdots & \ddots & \vdots \\ z_{N0} & z_{N1} & \cdots & z_{NN} \end{pmatrix}\begin{pmatrix} I_0 \\ I_1 \\ \vdots \\ I_N \end{pmatrix} = \begin{pmatrix} V(f) \\ 0 \\ \vdots \\ 0 \end{pmatrix}. \tag{10}$$

The input impedance calculation increases the computation time and may introduce an additional error in the solution. In this study, we use a current source to excite the wire antenna, so that (10) reduces to

$$\begin{pmatrix} z_{00} & z_{01} & \cdots & z_{0N} \\ z_{10} & z_{11} & \cdots & z_{1N} \\ \vdots & \vdots & \ddots & \vdots \\ z_{N0} & z_{N1} & \cdots & z_{NN} \end{pmatrix}\begin{pmatrix} I_0 \\ I_1 \\ \vdots \\ I_N \end{pmatrix} = \begin{pmatrix} 0 \\ 0 \\ \vdots \\ 0 \end{pmatrix} \tag{11}$$

where I_0 is determined by the current source. In this case, there are $(N+1)$ equations with N unknowns. Consequently, (11) can be transformed into the following $N\times N$ linear matrix equation:

$$\begin{pmatrix} z_{11} & z_{21} & \cdots & z_{1N} \\ z_{21} & z_{22} & \cdots & z_{2N} \\ \vdots & \vdots & \ddots & \vdots \\ z_{N1} & z_{N2} & \cdots & z_{NN} \end{pmatrix}\begin{pmatrix} I_1 \\ I_2 \\ \vdots \\ I_N \end{pmatrix} = \begin{pmatrix} -z_{10}I_0 \\ -z_{20}I_0 \\ \vdots \\ -z_{N0}I_0 \end{pmatrix} \text{ or } \boldsymbol{ZI} = \boldsymbol{V} \tag{12}$$

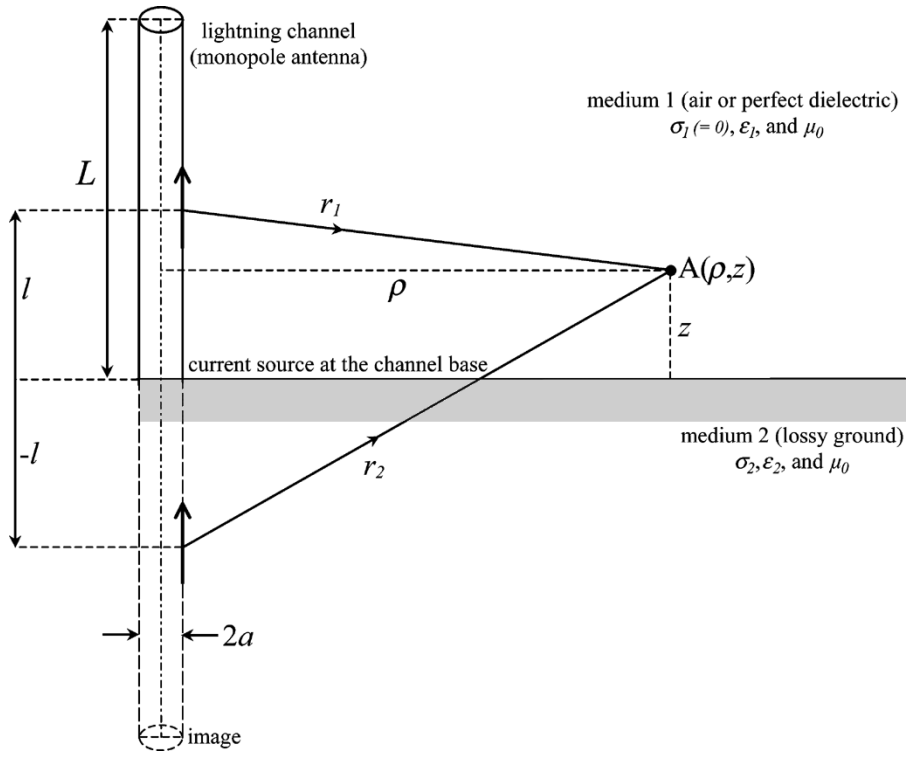

Fig. 4. Lightning channel above a lossy half-space.

where $z_{mn}(m, n = 1, 2 \dots N)$ are the mutual impedances between the sinusoidal dipoles defined as follows:

$$z_{mn} = \int_m F_m(l) E_n^t(l) dl \tag{13}$$

and $z_{m0}(m = 1, 2 \dots N)$ are the mutual impedances between the injection monopole and sinusoidal dipoles given as

$$z_{m0} = \int_m F_m(l) E_0^t(l) dl \tag{14}$$

where $E_n^t(l),\ n = 1, 2 \dots N$, and $E_0^t(l)$ are, respectively, the electric fields tangential to the wire surface due to the nth dipole (basis function) and the injection monopole. Also, $F_m(l)$ is the mth test dipole, and integrations are carried out over its length.

D. Lossy-Wire Antennas

Optical observations indicate that current waves are attenuated as they propagate along the lightning channel [47]. For the wire-monopole model of a lightning channel, attenuation due to the radiation losses is insufficient to reproduce such experimental observations [7], [8], [13], [14]. Thus, it is necessary to include distributed resistance R_D along the wire antenna, leading to the new impedance matrix given as [44]

$$Z_{mn} = z_{mn} \underbrace{- R_D \int_m F_m(l) H_n^{\varphi}(l) dl}_{z'_{mn}} \tag{15}$$

where $H_n^{\varphi}(l)$ is the azimuthal magnetic field due to the nth dipole, and z'_{mn} is the contribution to Z_{mn} from the distributed resistance. The introduction of distributed resistance requires modification of only diagonal and semi-diagonal elements in the impedance matrix [44]. Also, the limits of integral in the expression for z'_{mn} extend over two wire segments in the domain of test dipole $F_m(l)$.

Utilizing simplifying approximations, one can obtain [48]

$$H_n^{\varphi}(l) = \frac{F_n(l)}{2\pi a} \tag{16}$$

where a is the radius of wire antenna.

Hence

$$z'_{mn} = \frac{R_D}{2\pi a} \int_{m,n} F_n(l) F_m(l) dl \tag{17}$$

where region (m, n) is the wire surface shared by dipoles m and n. The expression for z'_{mn} reduces to [44]

$$z'_{mn} = \begin{cases} \frac{R_D}{4\pi\gamma a} \frac{\sinh(2\gamma d) - 2\gamma d}{\sinh^2(\gamma d)}, & \text{if (m=n)} \\ \frac{R_D}{4\pi\gamma a} \frac{\gamma d \cosh(\gamma d) - \sinh(\gamma d)}{\sinh^2(\gamma d)}, & \text{if } (m = n \pm 1) \\ 0, & \text{elsewhere.} \end{cases} \tag{18}$$

E. Lossy Half-Space Problem

Fig. 4 schematically shows a lightning channel above a lossy half-space. The thin-wire model of a lightning channel can be

considered as the superposition of infinitesimal dipoles. Electromagnetic radiation of a dipole above a lossy half-space was first investigated by Sommerfeld [31]. The approach involves semi-infinite integrals of Bessel functions that are characterized by highly oscillatory and weakly damping behavior. For very close observation points, various approximations have been proposed. In this paper, when evaluating elements of $\boldsymbol{Z}$ and $\boldsymbol{V}$ matrices in (12) for each sinusoidal dipole, its modified image is also included. Modified image theory was first introduced in [40]. As an illustration of this simple theory, consider a point current source placed in a dielectric medium above lossy ground (see Fig. 4). The field in the upper half-space (medium 1) is the superposition of contributions from the real source and its mirror image multiplied by a correction factor α_{11}, and the field in the lower half-space (medium 2) is due to the original source multiplied by a correction factor α_{12}. Applying the boundary conditions at the interface (i.e., the continuity of tangential electric field vector and scalar potential), one can obtain correction factors given by [40]

$$\begin{aligned}\alpha_{11} =& \frac{j\omega\varepsilon_1 - (\sigma_2 + j\omega\varepsilon_2)}{j\omega\varepsilon_1 + (\sigma_2 + j\omega\varepsilon_2)} \\ \alpha_{12} =& \frac{2(\sigma_2 + j\omega\varepsilon_2)}{j\omega\varepsilon_1 + (\sigma_2 + j\omega\varepsilon_2)}.\end{aligned} \tag{19}$$

Once $\boldsymbol{Z}$ and $\boldsymbol{V}$ are known, $\boldsymbol{I}$ can be determined from (12) utilizing a suitable solution of linear algebraic equations. The resultant current distribution can be used to calculate various field components in air. Since surface waves become significant as the observation point is moved farther from the source, the modified image theory is not applicable to distant field calculations. Thus, a different treatment is necessary. An accurate solution of this problem requires time-consuming evaluation of Sommerfeld integrals. For the situation examined here (the magnitude of the ground's complex wave number is much greater than that of free space), these integrals can be represented by closed-form expressions. In this regard, King [49] derived the complete expressions for electromagnetic fields of a vertical electric dipole over an imperfectly conducting (lossy) half-space. Also, King and Sandler [43] verified the suitability of these expressions for a dipole above certain types of lower half-space. The complete electromagnetic field expressions for a vertical straight wire antenna of length L above a lossy half-space for observation points in air (i.e., $\varepsilon_1 = \varepsilon_0$ in Fig. 4) are reproduced as

$$\begin{aligned}&H_{a\varphi}(\rho, z, j\omega) \\ &\quad = \int_0^L \frac{I_l(l)}{2\pi} \\ &\qquad \times \left[\frac{e^{-\gamma_1 r_1}}{2}\left(\frac{\rho}{r_1}\right)\left(\frac{1+\gamma_1 r_1}{r_1^2}\right)\right. \\ &\qquad\quad + \frac{e^{-\gamma_1 r_2}}{2}\left(\frac{\rho}{r_2}\right)\left(\frac{1+\gamma_1 r_2}{r_2^2}\right) \\ &\qquad\quad \left. - e^{-\gamma_1 r_2}\left(\frac{\gamma_1^3}{\gamma_2}\right)\left(\frac{\pi}{j\gamma_1\gamma_2}\right)^{\frac{1}{2}} e^{-jP} F(P)\right] dl\end{aligned} \tag{20}$$

$$\begin{aligned}&E_{a\rho}(\rho, z, j\omega) \\ &\quad = \frac{j\omega\mu_0}{2\pi\gamma_1}\int_0^L I_l(l) \\ &\qquad \times \left\{\frac{e^{-\gamma_1 r_1}}{2}\left(\frac{\rho}{r_1}\right)\left(\frac{z-l}{r_1}\right)\left(\frac{3+3\gamma_1 r_1+\gamma_1^2 r_1^2}{\gamma_1 r_1^3}\right)\right. \\ &\qquad\quad + \frac{e^{-\gamma_1 r_2}}{2}\left(\frac{\rho}{r_2}\right)\left(\frac{z+l}{r_2}\right)\left(\frac{3+3\gamma_1 r_2+\gamma_1^2 r_2^2}{\gamma_1 r_2^3}\right) \\ &\qquad\quad + \frac{\gamma_1}{\gamma_2} e^{-\gamma_1 r_2}\left[-\left(\frac{\rho}{r_2}\right)\left(\frac{1+\gamma_1 r_2}{r_2^2}\right)\right. \\ &\qquad\qquad \left.\left. + \frac{\gamma_1^3}{\gamma_2}\left(\frac{\pi}{j\gamma_1\gamma_2}\right)^{\frac{1}{2}} e^{-jP} F(P)\right]\right\} dl\end{aligned} \tag{21}$$

$$\begin{aligned}&E_{az}(\rho, z, j\omega) \\ &\quad = \frac{j\omega\mu_0}{2\pi\gamma_1}\int_0^L I_l(l) \\ &\qquad \times \left\{\frac{e^{-\gamma_1 r_1}}{2\gamma_1 r_1^3}\left[\left(1+\gamma_1 r_1+\gamma_1^2 r_1^2\right)\right.\right. \\ &\qquad\qquad \left. - \left(\frac{z-l}{r_1}\right)^2\left(3+3\gamma_1 r_1+\gamma_1^2 r_1^2\right)\right] \\ &\qquad\quad + \frac{e^{-\gamma_1 r_2}}{2\gamma_1 r_2^3}\left[\left(1+\gamma_1 r_2+\gamma_1^2 r_2^2\right)\right. \\ &\qquad\qquad \left. - \left(\frac{z+l}{r_2}\right)^2\left(3+3\gamma_1 r_2+\gamma_1^2 r_2^2\right)\right] \\ &\qquad\quad \left. - e^{-\gamma_1 r_2}\left(\frac{\gamma_1^3}{\gamma_2}\right)\left(\frac{\pi}{j\gamma_1\gamma_2}\right)^{\frac{1}{2}}\left(\frac{\rho}{r_2}\right) e^{-jP} F(P)\right\} dl\end{aligned} \tag{22}$$

where subscript a denotes observation points in air (not to be confused with radius a in Fig. 4 and in (16)–(18)), ω is the angular frequency, and (ρ, φ, z) are coordinates of the cylindrical coordinate system. Also, in (20)–(22)

$$\begin{aligned}\gamma_1 =& j\omega\sqrt{\mu_0\varepsilon_0} \\ \gamma_2 =& \sqrt{j\omega\mu_0(\sigma_2 + j\omega\varepsilon_2)}\end{aligned} \tag{23}$$

where ε_0 and μ_0 are free space permittivity and permeability, respectively, and

$$r_1 = \sqrt{\rho^2 + (z-l)^2}$$
$$r_2 = \sqrt{\rho^2 + (z+l)^2} \tag{24}$$

$$P = j\frac{\gamma_1^3 r_2}{2\gamma_2^2}\left[\frac{\gamma_1 r_2 + \gamma_2(z+l)}{\gamma_1\rho}\right]^2 \tag{25}$$

$$\begin{aligned}F(P) =& \frac{1}{\sqrt{2\pi}}\int_P^\infty \frac{e^{jz}}{\sqrt{z}} dz \\ =& \frac{1}{2}(1+j) - C_2(P) - jS_2(P)\end{aligned} \tag{26}$$

where $C_2(P)$ and $S_2(P)$ are, respectively, the Fresnel cosine and sine integrals of complex argument expressed as [50]

$$C_2(P) = \frac{1}{\sqrt{2\pi}} \int_0^P \frac{\cos z}{\sqrt{z}} dz$$

$$S_2(P) = \frac{1}{\sqrt{2\pi}} \int_0^P \frac{\sin z}{\sqrt{z}} dz. \tag{27}$$

Equations (20)–(22) are accurate everywhere in air or on the air–ground interface, provided that the following single condition is satisfied [49]:

$$|\gamma_2|^2 \gg |\gamma_1|^2 \quad \text{or} \quad |\gamma_2| \geq 3|\gamma_1|. \tag{28}$$

Each of the field expressions (20)–(22) contains three terms: a term in r_1, which is the direct wave from the source dipole, a similar term in r_2, which is the reflected wave from the image dipole, and a term containing $F(P)$ that involves Fresnel integrals, which is the surface or lateral wave. This surface wave is defined as the total field minus the perfect-ground approximation (geometrical-optics field), as opposed to the Zenneck surface wave (ZSW), which never exists as the sole contribution for the ground wave from a localized source [51]. Our surface wave might be considered as the Norton surface wave (NSW) [52], [53]. One can readily observe that field expressions (20)–(22) reduce to those based on the perfect-ground approximation when only the first two terms of each expression are retained.

For evaluation of $F(P)$, accurate series expansion of Fresnel integrals is used when $|P| < 4$. Under the condition of $|P| \geq 4$, the Fresnel integrals have asymptotic expansions that allow one to simplify the field expressions. Specifically

$$\frac{\gamma_1^3}{\gamma_2} \left(\frac{\pi}{j\gamma_1 r_2} \right)^{\frac{1}{2}} e^{-jP} F(P) \xrightarrow{|P| \geq 4} \frac{\gamma_1^3}{\gamma_2} \left(\frac{\pi}{j\gamma_1 r_2} \right)^{\frac{1}{2}} \frac{1}{(2\pi P)^{\frac{1}{2}}} \left(\frac{1}{2P} + j \right). \tag{29}$$

While most of the conventional methods (e.g., [26] and [27]) use different treatments for the two (ρ and z) components of electric field, the closed-form electric field expressions (21) and (22) employed here are parts of the same solution. Also, the magnetic field component given by (20) is obtained using the same methodology. It is shown in the Appendix that the Cooray–Rubinstein formula for the horizontal (ρ) electric field component is a special case of (21) when the term containing Fresnel integrals is neglected.

III. Numerical Analysis and Results

A. Specification of the Problem

The thin-wire antenna model of lightning channel above a lossy ground is illustrated in Fig. 4. The antenna has length $L = 2600$ m, radius $a = 0.05$ m, and distributed resistance $R_D = 0.1\ \Omega$/m. It is driven at its bottom end by a current source whose waveform is the same as that used in [2], [4], [7], and in other studies. This waveform (Fig. 5) is characterized by a peak value of about 11 kA and a peak current rate of rise of about 105 kA/μs. In finding the distribution of current along the antenna, $\varepsilon_1 = 5.3\varepsilon_0$ is set for the ambient medium in order to obtain a current wave propagation velocity of 1.3×10^8 m/s [7]. This value of permittivity was used for the upper medium (medium 1) in (19), in the procedure to account for the effect of lossy ground. Then, as mentioned earlier, the resultant current waveforms were used in field expressions (20)–(22) to calculate remote field components above a lossy ground assuming $\varepsilon_1 = \varepsilon_0$ (i.e., assuming that medium 1 is air or free space).

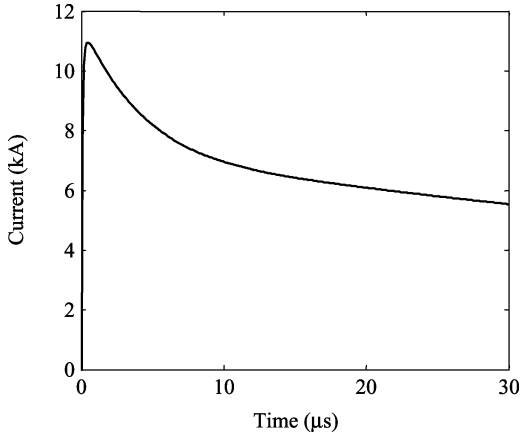

Fig. 5. Channel-base current used for comparison of the AT models.

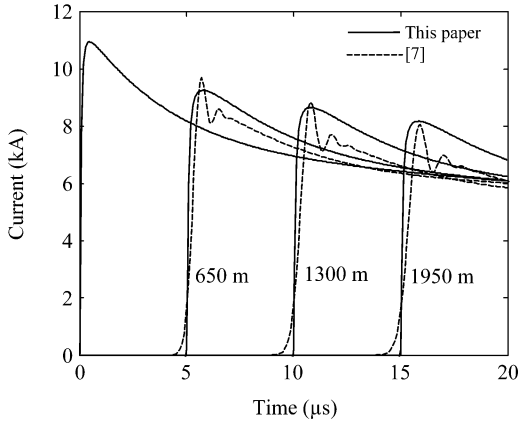

Fig. 6. Current waveforms at three heights: 650, 1300, and 1950 m.

Frequency-domain calculations are carried out at 8192 frequencies up to 10 MHz with frequency intervals of 2.44 kHz. This corresponds to a sampling interval of 0.05 μs over a time window of 409.6 μs. To ensure the convergence of the MoM, the smallest segment length should not exceed one fourth of the minimum wavelength. We divided the 2600-m wire representing the lightning channel into 800 segments, each 3.25 m in length.

B. Comparison With the AT Model Presented in [7]

1) Current Distributions: The current source excitation of the antenna is implemented by using a Dirac delta source [15], [16] connected across a 3.25-m gap, whereas in the AT model described in [7] a voltage source (delta-gap generator) was connected across the gap. There are some differences between the two excitation methods. For example, the channel-base current

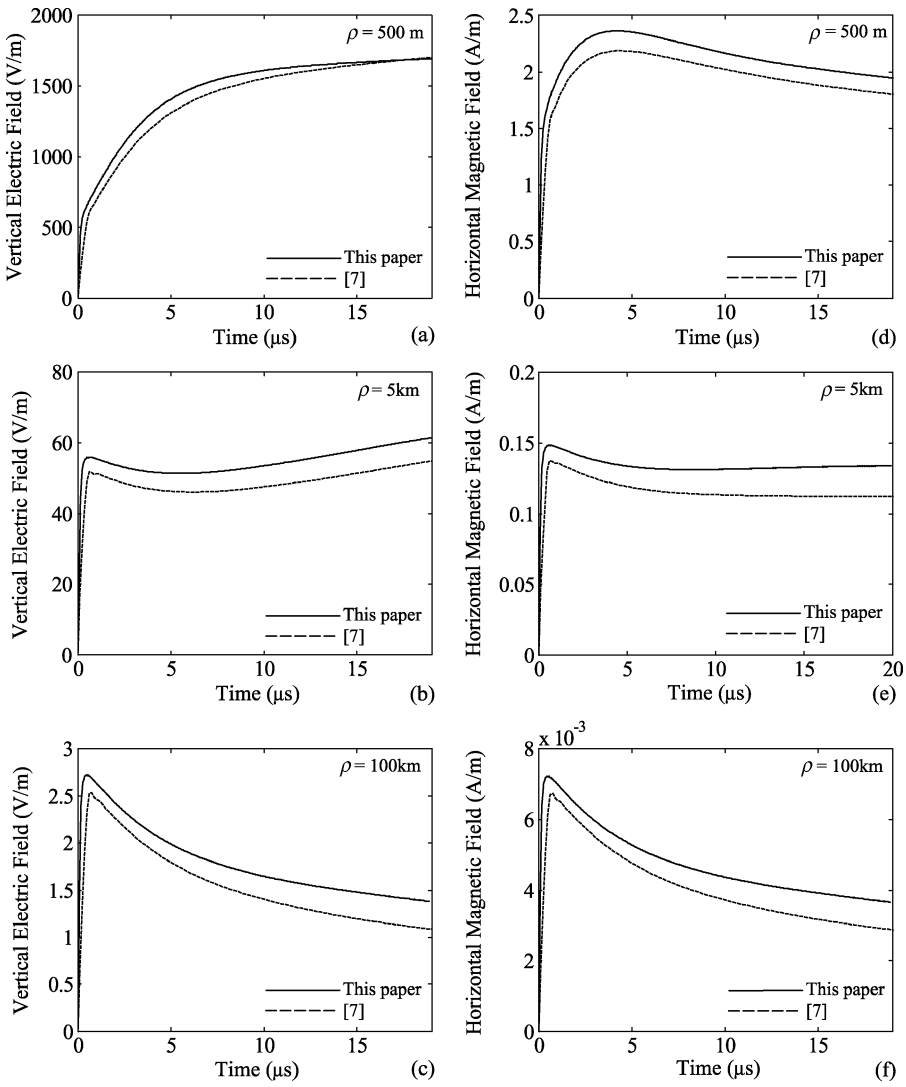

Fig. 7. (a)–(c) Vertical electric and (d)–(f) horizontal magnetic fields at the air–ground interface 500 m, 5 km, and 100 km from the lightning channel base for a perfect ground computed using the model proposed in this paper and the AT model described in [7].

remains unchanged upon the arrival of a wave reflected from the wire top end in the case of current excitation, although we consider the times before the arrival of the first reflection from the top. This is not the case when voltage excitation is used. Also, the antenna theory model proposed here solves a modified version of the EFIE for space–time-dependent currents with the excitation being the current source. Direct use of channel-base current in the method of moments (MoM) eliminates preliminary steps, including calculation of antenna's input impedance, and improves the method's reliability.

To demonstrate the capabilities of the proposed model, it is compared with the AT model described in [7] for the case of a perfectly conducting ground. Current distributions obtained using the two models are presented in Fig. 6 as a function of time at heights of 650, 1300, and 1950 m from the channel base. It is worth mentioning that the plots for the AT model described in [7] show oscillations around the current peak. These are due to the numerical instabilities and could be eliminated by increasing the computation accuracy (see, for example, [13]). Like the AT model described in [7], the proposed model predicts attenuation and dispersion of the current pulse as it propagates along the lightning channel. Note that the observed variation of current with height follows from the solution of Maxwell's equations, in contrast with the commonly used engineering models in which imposed current distributions are used. A detailed comparison between the AT model and commonly used engineering models is found in [7].

2) Electromagnetic Fields: Fig. 7(a)–(f) depicts electric and magnetic fields predicted by the two models at different distances from the channel base on a perfectly conducting ground. As seen in this figure, except for relatively small differences in the values of the field amplitude and rise time, the results predicted by the two models are similar. The differences between field amplitudes predicted by the two models may be related to the differences between current waveforms of the two models that are mainly due to the different techniques implemented for the solution of the EFIE in the time and frequency domains. Also, differences between the rise times of field waveforms are thought to be due to numerical instabilities in the AT model described in [7].

When the electromagnetic field features tabulated in [1] and [14] are considered as a benchmark, both models reproduce all

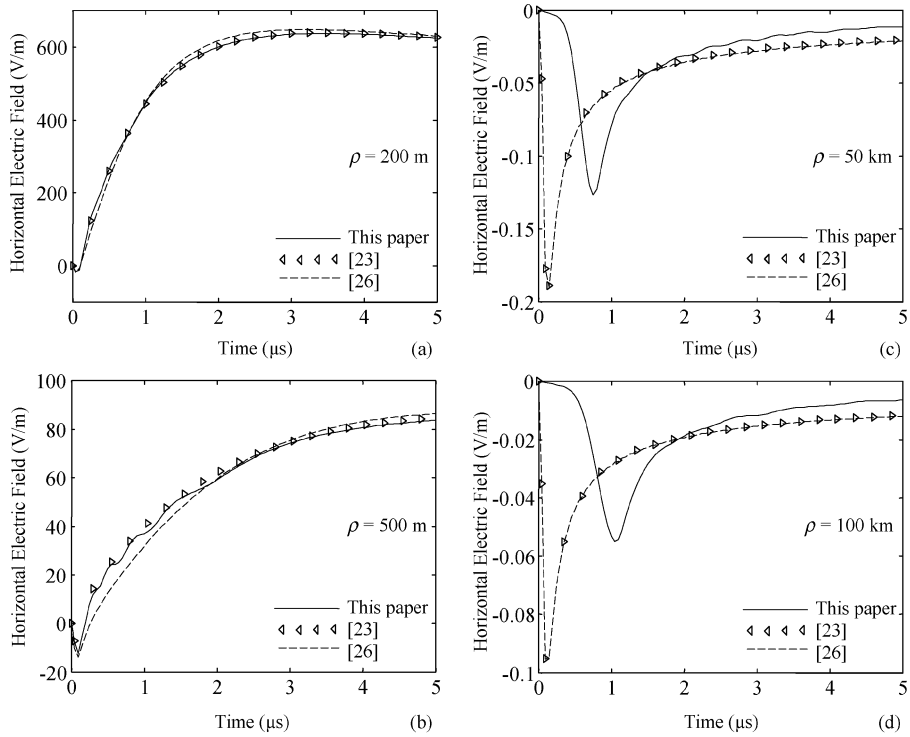

Fig. 8. Horizontal electric field at a 20-m height above ground with conductivity $\sigma_2 = 0.04$ S/m and permittivity $\varepsilon_2 = 8\,\varepsilon_0$ computed using the approach of this paper, the Cooray–Rubinstein formula, and the Cooray modified formula: (a) 200 m, (b) 500 m, (c) 50 km, and (d) 100 km from the lightning channel base displayed on a 5-μs time scale.

known characteristic features except for the hump following the initial peak in far magnetic fields and zero crossing in both electric and magnetic fields at far ranges.

C. Electromagnetic Fields Above Lossy Half-Space

1) Horizontal Electric Field: In studies of the coupling of lightning-radiated electromagnetic fields to overhead power lines, it is convenient to use the horizontal component of the electric field [24], [55]. Up to now, the Cooray–Rubinstein formula [23] or the Cooray modified formula [26] have probably been the best simple approximations presented for the calculation of horizontal electric field. For convenience, we rewrite the Cooray–Rubinstein formula as follows:

$$E_{a\rho}(\rho,z,j\omega) = E_{a\rho p}(\rho,z,j\omega) - \sqrt{\frac{j\omega\mu_0}{\sigma_2 + j\omega\varepsilon_2}}\,H_{a\varphi p}(\rho,0,j\omega) = E_{a\rho p}(\rho,z,j\omega) + E_{a\rho}(\rho,0,j\omega) \quad (30)$$

where ρ is the radial distance from the channel base, z is the height above ground, and subscript p denotes the perfect-ground assumption (see Fig. 4). Cooray [26] proposed a modification to the first term in (30) weakening the contribution of its radiation component

$$E_{a\rho}(\rho,z,j\omega) = 0.4E_{a\rho p,r}(\rho,z,j\omega) + E_{a\rho p,i}(\rho,z,j\omega) + E_{a\rho p,s}(\rho,z,j\omega) + E_{a\rho}(\rho,0,j\omega) \quad (31)$$

where $E_{a\rho p,r}$, $E_{a\rho p,i}$, and $E_{a\rho p,s}$ are, respectively, the radiation, induction, and static terms of $E_{a\rho p}(\rho,z,j\omega)$ in (30). In fact, in the expression for horizontal electric field above a perfect ground, $E_{a\rho p,r}$ is the term with $1/r^3$ dependence, $E_{a\rho p,i}$ is the term with $1/r^4$ dependence, and $E_{a\rho p,s}$ is the term with $1/r^5$ dependence. Although this approach predicts a more accurate initial peak of the horizontal electric field at near ranges, it is not applicable to the case of perfect ground [26].

Horizontal electric field waveforms at a 20-m height above ground with conductivity $\sigma_2 = 0.04$ S/m and permittivity $\varepsilon_2 = 8\,\varepsilon_0$ for different distances from the channel base are shown (on a 5-μs time scale) in Fig. 8(a)–(d). Fields are obtained using the method presented in this paper, the Cooray–Rubinstein formula [23], and the Cooray modified formula [26]. It is clearly seen from Fig. 8 that, at near ranges (e.g., 200 m), most important in studying lightning-induced overvoltages on power distribution lines, the fields predicted by these three methods are in close agreement. When the observation point is moved to intermediate and far ranges (e.g., 100 km), differences between the approach of this paper and the Cooray–Rubinstein or Cooray modified formulas become considerable. It is worth mentioning that, at far ranges, the Cooray–Rubinstein and the Cooray modified formulas yield results that are very close to those predicted by the wavetilt formula. It can be analytically shown that, for a far observation point a few tens of meters above ground, the Cooray–Rubinstein (or Cooray modified) formula approximately reduces to the wavetilt expression [23], [51]. At far ranges, the limiting case of the Cooray–Rubinstein and wavetilt formulas is indeed exact if one deals with a pure Zenneck surface wave. However, such never exists as the only contribution from a localized source [51]. It follows from Fig. 8 that the surface wave component, which in our approach is not necessarily the Zenneck surface wave, is not adequately accounted for in the Cooray–Rubinstein, Cooray modified, and wavetilt formulas. While the term containing Fresnel integrals (the Fresnel term)

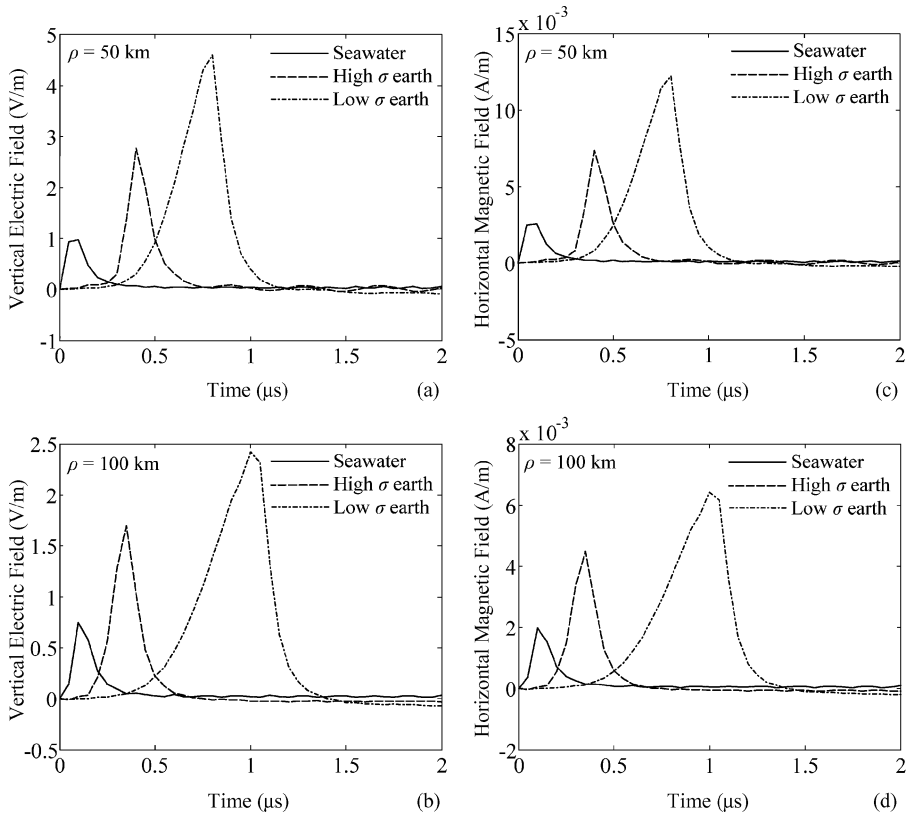

Fig. 9. Surface wave components of the (a), (b) vertical electric and (c), (d) horizontal magnetic fields computed at the air–ground interface for three types of the lower half-space 50 and 100 km from the lightning channel-base displayed on a 2-μs time scale.

is negligible at near ranges, it becomes significant at intermediate and far ranges. For convenience, we rewrite the surface wave component of the horizontal electric field [the terms in the brackets in (21)] as follows:

$$E_{a\rho s}(\rho,z,j\omega) = -\frac{j\omega\mu_0}{2\pi\gamma_1}\int_0^L I_l(l)\left[\frac{\gamma_1}{\gamma_2}e^{-\gamma_1 r_2}\left(\frac{\rho}{r_2}\right)\left(\frac{1+\gamma_1 r_2}{r_2^2}\right)\right]dl + \frac{j\omega\mu_0}{2\pi\gamma_1}\int_0^L I_l(l)\left[e^{-\gamma_1 r_2}\frac{\gamma_1^4}{\gamma_2^2}\left(\frac{\pi}{j\gamma_1\gamma_2}\right)^{\frac{1}{2}}e^{-jP}F(P)\right]dl \quad (32)$$

where subscript s denotes the surface wave. Only the first term of (32) is included in the Cooray–Rubinstein formula. As Fig. 8 indicates, the difference between the results of this paper and those predicted by Cooray–Rubinstein and Cooray modified formulas at distant points is more pronounced at early times and gradually diminishes at later times. Further, for high values of ground's conductivity and permittivity, our approach, the Cooray–Rubinstein formula, and the Cooray modified formula (and even the wavetilt formula for remote observation points a few tens of meters above ground) all predict similar fields, since the Fresnel term in this case is very small.

2) Surface Waves: We now consider three practical cases of the lower half-space, seawater, relatively high conductivity earth, and relatively low conductivity earth. The constitutive parameters for these cases are given in Table I and are similar to those given in [43]. Fig. 9(a)–(d) illustrates contributions of the surface waves to the vertical electric and horizontal magnetic fields. In order to better resolve all significant features of the waveforms occurring at early times, only the first 2 μs are shown. Calculations were carried out at the air–ground interface at two distances: 50 and 100 km from the channel base. Waveforms shown in this figure reveal four interesting features of surface waves.

1) Surface waves exhibit flattening after the rapid variation (sharp initial peak) during the first some hundreds of nanoseconds to 1 μs or so.
2) The amplitude of surface waves tends to decrease as the observation point is moved farther away from the source. This effect is most pronounced for relatively low conductivity earth.

TABLE I
CONSTITUTIVE PARAMETERS OF THREE REALISTIC CASES OF THE LOWER HALF-SPACE

Medium	σ_2, S/m	$\varepsilon_2/\varepsilon_0$
Seawater	4.0	80
Relatively high conductivity earth	0.4	12
Relatively low conductivity earth	0.04	8

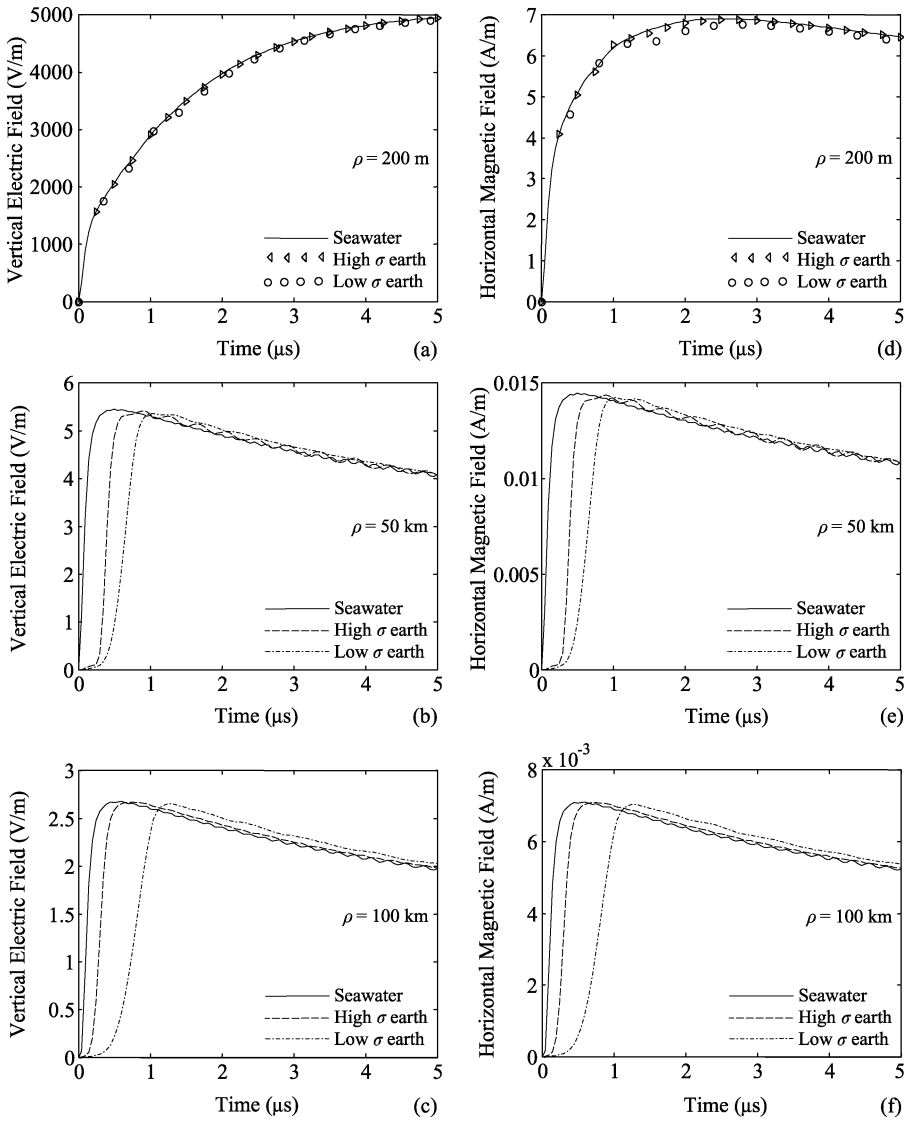

Fig. 10. (a)–(c) Vertical electric and (d)–(f) horizontal magnetic fields at the air–ground interface for three types of the lower half-space 200 m, 50 km, and 100 km from the lightning channel base displayed on a 5-μs time scale.

3) For a given observation point, surface waves become more pronounced as the conductivity of the lower half-space decreases.
4) For a given observation point, surface waves exhibit more gradual rise to peak as the conductivity of the lower half-space decreases.

Fig. 9 also shows that the initial rise time of each field component increases as the observation point is moved farther away from the channel base. It appears that neglecting surface waves, as is commonly done in the calculation of lightning-radiated electromagnetic fields, is only justified when the lower half-space has relatively high conductivity.

3) Total Electric and Magnetic Fields: The conductivity of the lower half-space could strongly influence the characteristics of lightning-radiated fields. Field components suffer from propagation effects as they travel along the interface. The lossy interface preferentially attenuates higher frequency components of radiated electric and magnetic fields, which results in an increase in the rise time and a decrease in the magnitude. These effects are illustrated in Fig. 10(a)–(f). Calculations were performed for three types of the lower half-space: sea water, relatively high conductivity earth, and relatively low conductivity earth at distances of 200 m, 50 km, and 100 km from the lightning channel base. The computed field waveforms are displayed on a 5-μs time scale. Fig. 11(a)–(c) depicts horizontal electric fields for the same conditions as in Fig. 10. As seen from these figures, as the lower half-space becomes less conductive, distortions in the radiated vertical electric, horizontal electric, and horizontal magnetic fields become more significant, and the horizontal electric field becomes larger. The results of this study indicate that, in the analysis of lightning-radiated electromagnetic fields over practical lower half-spaces, the perfect-ground assumption yields results that may differ considerably from those predicted by the more realistic approach described here, particularly at greater distances from the lightning channel.

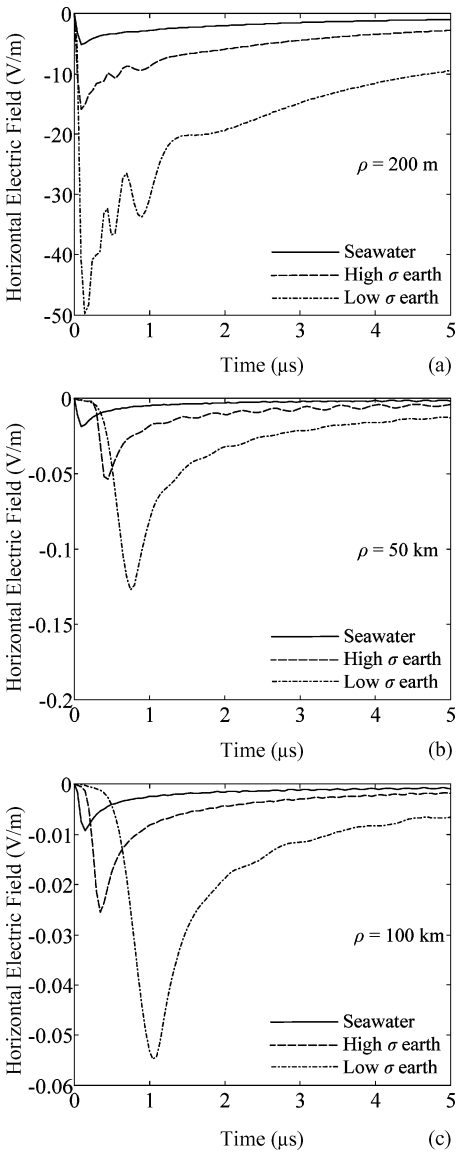

Fig. 11. Horizontal electric fields at the air–ground interface for three types of the lower half-space (a) 200 m, (b) 50 km, and (c) 100 km from the lightning channel-base displayed on a 5-μs time scale.

We now discuss the polarity of the horizontal electric field as a function of distance. The results of Fig. 11 reveal that, for the three types of the lower half-space, the horizontal electric field at the air–ground interface exhibits the same (negative) polarity for the entire range of distances (200 m to 100 km) considered. This is in contrast with the results of Fig. 8 where the horizontal electric field waveforms are shown for observation points at a height of 20 m above ground. In this latter case, the horizontal electric field exhibits predominantly positive polarity at close distances and negative polarity at far distances. Such a dissimilarity is due to the difference in height of the observation point above ground. In the Cooray–Rubinstein expression for the horizontal electric field (30) or in the expression proposed in this paper, the contribution from the first term (i.e., the horizontal electric field corresponding to the perfect-ground assumption) has positive polarity [23], while the remainder of the expression has negative polarity. The former dominates at near observation points a few tens of meters above ground, resulting in the positive polarity of the total horizontal electric field. The contribution from the remainder of the field expression becomes dominant as the observation point moves toward the air–ground interface or farther away from the channel-base. Consequently, when the observation point is at the air–ground interface or at a large distance, the total horizontal electric field has negative polarity.

The oscillations seen in Figs. 10(d) and 11(a) during the initial 2 μs of field waveforms for relatively low-conductivity earth 200 m from the channel base are related to the oscillatory behavior of Fresnel integrals of complex argument.

IV. Conclusion

A new AT model has been used to compute the lightning return stroke current distribution along the channel and resultant remote electromagnetic fields. In this model, the return-stroke channel is represented by a lossy vertical wire antenna above ground. A current source is used for the excitation of the wire in order to eliminate the antenna's input impedance calculations required in the AT model described in [7]. The model can reproduce all electromagnetic field benchmark features used for model evaluation, except for the hump following the initial peak in magnetic fields and zero crossing in both electric and magnetic fields at far ranges. The finite conductivity of lower half-space is accounted for in computing lightning-radiated electromagnetic fields by including a surface wave component. It has been shown that the Cooray–Rubinstein formula for calculation of the horizontal electric field is an approximation that becomes inadequate at far ranges and for poorly conducting ground. Complete electromagnetic fields over lossy ground are analyzed, and it has been shown that the rise time and peak value of both electric and magnetic fields are significantly influenced by propagation over a poorly conducting ground. A decrease in ground conductivity results in an increase in rise time and a decrease in magnitude of the field. Overall, the results suggest that the neglecting of the influence of ground's finite conductivity is not acceptable in most practical situations.

Appendix
Derivation of the Cooray–Rubinstein Formula From the Formulation of This Paper

Considering only the first two terms in (20) and (21) yields the horizontal magnetic and horizontal electric field components, respectively, corresponding to the perfect-ground assumption (denoted by subscript p) as follows:

$$H_{a\varphi p}(\rho,z,j\omega) = \int_0^L \frac{I_l(l)}{2\pi}\left[\frac{e^{-\gamma_1 r_1}}{2}\left(\frac{\rho}{r_1}\right)\left(\frac{1+\gamma_1 r_1}{r_1^2}\right) + \frac{e^{-\gamma_1 r_2}}{2}\left(\frac{\rho}{r_2}\right)\left(\frac{1+\gamma_1 r_2}{r_2^2}\right)\right] dl \quad \text{(A1)}$$

$$E_{a\rho p}(\rho,z,j\omega) = \frac{j\omega\mu_0}{2\pi\gamma_1}\int_0^L I_l(l) \times\left\{\frac{e^{-\gamma_1 r_1}}{2}\left(\frac{\rho}{r_1}\right)\left(\frac{z-l}{r_1}\right)\left(\frac{3+3\gamma_1 r_1+\gamma_1^2 r_1^2}{\gamma_1 r_1^3}\right) + \frac{e^{-\gamma_1 r_2}}{2}\left(\frac{\rho}{r_2}\right)\left(\frac{z+l}{r_2}\right) \times\left(\frac{3+3\gamma_1 r_2+\gamma_1^2 r_2^2}{\gamma_1 r_2^3}\right)\right\} dl. \quad \text{(A2)}$$

Consequently, (21) can be expressed as follows:

$$\begin{aligned} E_{a\rho}(\rho,z,j\omega) &= E_{a\rho p}(\rho,z,j\omega) + \frac{j\omega\mu_0}{2\pi\gamma_1}\int_0^L I_l(l) \times\left\{\frac{\gamma_1}{\gamma_2}e^{-\gamma_1 r_2}\left[-\left(\frac{\rho}{r_2}\right)\left(\frac{1+\gamma_1 r_2}{r_2^2}\right) + \frac{\gamma_1^3}{\gamma_2}\left(\frac{\pi}{j\gamma_1\gamma_2}\right)^{\frac{1}{2}} e^{-jP}F(P)\right]\right\} dl \\ &= E_{a\rho p}(\rho,z,j\omega) - \frac{j\omega\mu_0}{\gamma_1} \times\int_0^L \frac{I_l(l)}{2\pi}\left\{\frac{\gamma_1}{\gamma_2}e^{-\gamma_1 r_2}\left[\left(\frac{\rho}{r_2}\right)\left(\frac{1+\gamma_1 r_2}{r_2^2}\right)\right]\right\} dl + \frac{j\omega\mu_0}{2\pi\gamma_1} \times\int_0^L I_l(l)\left\{e^{-\gamma_1 r_2}\frac{\gamma_1^4}{\gamma_2^2}\left(\frac{\pi}{j\gamma_1\gamma_2}\right)^{\frac{1}{2}} e^{-jP}F(P)\right\} dl. \end{aligned} \quad \text{(A3)}$$

If the observation point is on the interface (i.e., $z=0$ and $r_1 = r_2$), then (A1) can be reduced as follows:

$$H_{a\varphi p}(\rho,0,j\omega) = \int_0^L \frac{I_l(l)}{2\pi}e^{-\gamma_1 r_2}\left[\left(\frac{\rho}{r_2}\right)\left(\frac{1+\gamma_1 r_2}{r_2^2}\right)\right] dl. \quad \text{(A4)}$$

Applying (A4) to the second term of (A3) and dropping the third term [containing $F(P)$ and, hence, Fresnel integrals given by (27)] of (A3), we obtain

$$\begin{aligned} E_{a\rho}(\rho,z,j\omega) &= E_{a\rho p}(\rho,z,j\omega) - \frac{j\omega\mu_0}{\gamma_2}H_{a\varphi p}(\rho,0,j\omega) \\ &= E_{a\rho p}(\rho,z,j\omega) - \sqrt{\frac{j\omega\mu_0}{\sigma_2+j\omega\varepsilon_2}}H_{a\varphi p}(\rho,0,j\omega) \end{aligned} \quad \text{(A5)}$$

which is identical to (30), the Cooray–Rubinstein formula.

Thus, the Cooray–Rubinstein formula is an approximation that neglects the last term of (A3). The approximation is valid for near ranges but becomes inadequate for intermediate and far ranges (see Fig. 8).

ACKNOWLEDGMENT

The authors would like to thank Y. Baba, F. Rachidi, and two anonymous reviewers for providing useful comments on the paper.

REFERENCES

[1] V. A. Rakov and M. A. Uman, "Review and evaluation of lightning return stroke models including some aspects of their application," *IEEE Trans. Electromagn. Compat.*, vol. 40, no. 4, pp. 403–426, Nov. 1998.

[2] C. A. Nucci, G. Diendorfer, M. A. Uman, F. Rachidi, M. Ianoz, and C. Mazzetti, "Lightning return stroke current models with specified channel base current: a review and comparison," *J. Geophys. Res.*, vol. 95, pp. 20 395–20 408, Nov. 1990.

[3] R. Thottappillil and M. A. Uman, "Comparison of lightning return-stroke models," *J. Geophys. Res.*, vol. 98, pp. 22 903–22 914, Dec. 1993.

[4] R. Thottappillil, V. A. Rakov, and M. A. Uman, "Distribution of charge along the lightning channel: relation to remote electric and magnetic fields and to return stroke models," *J. Geophys. Res.*, vol. 102, pp. 6887–7006, 1997.

[5] V. A. Rakov, "Lightning return stroke modeling: recent developments," in *Proc. 3rd Brazilian Workshop Atmospheric Electricity/Int. Conf. Grounding and Earthing*, Rio de Janeiro, Brazil, Nov. 2002, pp. 85–96.

[6] ——, "Engineering models of the lightning return stroke," in *Proc. Int. Symp. Lightning Protection (VII SIPDA)*, Curitiba, Brazil, Nov. 2003, pp. 511–530.

[7] R. Moini, B. Kordi, G. Z. Rafi, and V. A. Rakov, "A new lightning return stroke model based on antenna theory model," *J. Geophys. Res.*, vol. 105, no. D24, pp. 29 693–29 702, Dec. 2000.

[8] Y. Baba and M. Ishii, "Numerical electromagnetic field analysis of lightning current in tall structures," *IEEE Trans. Power Del.*, vol. 16, no. 2, pp. 324–328, Apr. 2001.

[9] B. Kordi, R. Moini, and V. A. Rakov, "Comment on "Return stroke transmission line model for stroke speed near and equal that of light," by R. Thottappillil, J. Schoene, and M. A. Uman," *Geophys. Res. Lett.*, vol. 29, no. 10, p. 1369, 2002.

[10] S. Visacro, A. Soares, and A. A. O. Schroeder, "An interactive computational code for simulation of transient behavior of electric system components for lightning currents," in *Proc. 26th Int. Conf. Lightning Protection*, Cracow, Poland, 2002, pp. 732–737.

[11] S. Visacro and F. H. Silveira, "Evaluation of current distribution along the discharge channel by an electromagnetic model," in *Proc. 26th Int. Conf. Lightning Protection*, Cracow, Poland, 2002, pp. 42–45.

[12] G. Maslowski, "Influence of lightning branches and channel inclination on the lightning electromagnetic fields," in *Proc. Int. Carpathian Conf. Electromagn. Compat.*, Rzeszow-Lancut, Poland, 2002, pp. IV.3-1–IV.3-6.

[13] B. Kordi, R. Moini, and V. A. Rakov, "Comparison of lightning return stroke electric fields predicted by the transmission line and antenna theory models," in *Proc. 15th Int. Zurich Symp. Electromagn. Compat.*, Zurich, Switzerland, Feb. 2003, pp. 551–556.

[14] Y. Baba and M. Ishii, "Characteristics of electromagnetic return-stroke models," *IEEE Trans. Electromagn. Compat.*, vol. 45, no. 1, pp. 129–135, Feb. 2003.

[15] A. Shoory, R. Moini, and S. H. H. Sadeghi, "Analysis of lightning electromagnetic fields in the vicinity of a lossy ground, using a new antenna theory model," in *Proc. IEEE Bologna PowerTech., CD Rom*, Bologna, Italy, Jun. 2003.

[16] L. Grcev, F. Rachidi, and V. A. Rakov, "Comparison of electromagnetic models of lightning return strokes using current and voltage sources," in *Proc. 12th Int. Conf. Atmospheric Electricity*, Versailles, France, 2003, pp. 593–596.

[17] Y. Baba and V. A. Rakov, "On the transmission line model for lightning return stroke representation," *Geophys. Res. Lett.*, vol. 30, no. 24, p. 2294, 2003.

[18] B. Kordi, R. Moini, W. Janischewskyj, A. M. Hussein, V. Shostak, and V. A. Rakov, "Application of the antenna theory model to a tall tower struck by lightning," *J. Geophys. Res.*, vol. 108, no. D17, p. 4542, 2003.

[19] G. J. Burke and A. J. Poggio, "Numerical Electromagnetic Code (NEC)-Method of Moments," Naval Ocean System Center, San Diego, CA, Tech. Document 116, Jan. 1980.
[20] J. Zenneck, *Wireless Telegraphy*. New York: McGraw-Hill, 1915.
[21] M. J. Master and M. A. Uman, "Lightning induced voltages on power lines: theory," *IEEE Trans. Power App. Syst.*, vol. PAS-103, pp. 2502–2518, Sep. 1984.
[22] V. Cooray, "Horizontal fields generated by return strokes," *Radio Sci.*, vol. 27, pp. 529–537, Jul.–Aug. 1992.
[23] M. Rubinstein, "An approximate formula for the calculation of the horizontal electric field from lightning at close, intermediate, and long ranges," *IEEE Trans. Electromagn. Compat.*, vol. 38, no. 3, pp. 531–535, Aug. 1996.
[24] F. Rachidi, C. A. Nucci, M. Ianoz, and C. Mazzetti, "Influence of a lossy ground on lightning-induced voltages on overhead lines," *IEEE Trans. Electromagn. Compat.*, vol. 38, no. 3, pp. 250–264, Aug. 1996.
[25] J. R. Wait, "Concerning the horizontal electric field of lightning," *IEEE Trans. Electromagn. Compat.*, vol. 39, no. 2, p. 186, May 1997.
[26] V. Cooray, "Some considerations on the Cooray-Rubinstein formulation used in deriving the horizontal electric field of lightning return strokes over finitely conducting ground," *IEEE Trans. Electromagn. Compat.*, vol. 44, no. 4, pp. 560–566, Nov. 2002.
[27] V. Cooray and S. Lundquist, "Effects of propagation on the rise times and the initial peaks of radiation fields from return strokes," *Radio Sci.*, vol. 22, pp. 409–415, 1983.
[28] M. Fernando and V. Cooray, "The peak, rise time and the half-width of lightning generated electromagnetic field derivatives over finitely conducting ground," in *Proc. IEE 10th Int. Conf. Electromagn. Compat.*, Sep. 1997, pp. 158–163.
[29] J. R. Wait, "Transient fields of a vertical dipole over a homogeneous curved ground," *Can. J. Phys.*, vol. 34, pp. 27–35, 1956.
[30] V. Cooray, "Underground electromagnetic fields generated by the return strokes of lightning flashes," *IEEE Trans. Electromagn. Compat.*, vol. 43, no. 1, pp. 75–84, Feb. 2001.
[31] A. Sommerfeld, "Uber die ausbreitung der Wellen in der drahtlosen Telegraphie," *Ann. Phys.*, vol. 28, p. 665, 1909.
[32] A. Banos, *Dipole Radiation in the Presence of a Conducting Half-Space*. New York: Pergamon, 1966.
[33] W. C. Kuo and K. K. Mei, "Numerical approximations of Sommerfeld integrals for fast convergence," *Radio Sci.*, vol. 13, no. 3, pp. 407–415, May–Jun. 1978.
[34] P. Parhami, Y. Rahmat-Samii, and R. Mitra, "An efficient approach for evaluating Sommerfeld integrals encountered in the problem of a current element radiating over lossy ground," *IEEE Trans. Antennas Propagat.*, vol. AP-28, no. 1, pp. 100–104, Jan. 1980.
[35] K. A. Norton, "Propagation of radio waves over the surface of the earth and in the upper atmosphere, II," *Proc. Inst. Radio Eng.*, vol. 25, no. 9, pp. 1203–1236, Sep. 1937.
[36] A. Zeddam and P. Degauque, "Current and voltage induced on telecommunications cable by a lightning return stroke," in *Lightning Electromagnetics*, R. L. Gardner, Ed. New York: Hemisphere, 1990, pp. 377–400.
[37] T. J. Cui and W. C. Chew, "Modeling of arbitrary wire antennas above ground," *IEEE Trans. Geosci. Remote Sens.*, vol. 38, no. 1, pp. 357–365, Jan. 2000.
[38] ——, "Accurate model of arbitrary wire antennas in free space, above or inside ground," *IEEE Trans. Antennas Propagat.*, vol. 48, no. 4, pp. 482–493, Apr. 2000.
[39] ——, "Accurate analysis of wire structures from very-low frequency to microwave frequency," *IEEE Trans. Antennas Propagat.*, vol. 50, no. 3, pp. 301–307, Mar. 2002.
[40] T. Takashima, T. Nakae, and R. Ishibashi, "Calculation of complex fields in conducting media," *IEEE Trans. Electr. Insul.*, vol. EI-15, pp. 1–7, 1980.
[41] L. Grcev, "Computation of transient voltages near complex grounding systems caused by lightning currents," in *Proc. IEEE Int. Symp. Electromagn. Compat.*, 1992, 92CH3169-0, pp. 393–400.
[42] ——, "Computer analysis of transient voltages in large grounding systems," *IEEE Trans. Power Del.*, vol. 11, no. 2, pp. 815–823, Apr. 1996.
[43] R. W. P. King and S. S. Sandler, "The electromagnetic field of a vertical electric dipole over the earth or sea," *IEEE Trans. Antennas Propagat.*, vol. 42, no. 3, pp. 382–389, Mar. 1994.
[44] J. H. Richmond, "Radiation and scattering by thin-wire structures in the complex frequency domain," in *Computational Electromagnetics*, E. K. Miller, Ed. New York: IEEE Press, 1992.
[45] S. A. Schelkunoff and H. T. Friis, *Antennas, Theory and Practice*. New York: Wiley, 1952, pp. 370–401.
[46] D. V. Otto and J. H. Richmond, "Rigorous field expressions for piecewise-sinusoidal line sources," *IEEE Trans. Antennas Propagat.*, vol. AP-17, no. 1, p. 98, Jan. 1969.
[47] V. A. Rakov and M. A. Uman, *Lightning: Physics and Effects*. Cambridge, U.K.: Cambridge Univ. Press, 2003.
[48] J. A. Stratton, *Electromagnetic Theory*. New York: McGraw-Hill, 1941.
[49] R. W. P. King, "Electromagnetic field of a vertical electric dipole over an imperfectly conducting half-space," *Radio Sci.*, vol. 25, pp. 149–160, Mar.–Apr. 1990.
[50] M. Abramowitz and I. Stegun, *Handbook of Mathematical Functions*. New York: Dover, 1970.
[51] J. R. Wait, "On the wavetilt at high frequencies-a personal view," *IEEE Trans. Electromagn. Compat.*, vol. 39, no. 1, p. 65, Feb. 1997.
[52] ——, "The ancient and modern history of EM ground-wave propagation," *IEEE Antennas Propagat. Mag.*, vol. 40, no. 5, pp. 7–24, Oct. 1998.
[53] ——, *Electromagnetic Waves in Stratified Media*. New York: IEEE Press, 1996.
[54] R. W. P. King, "On the radiation efficiency and the electromagnetic field of a vertical electric dipole in the air above a dielectric or conducting half-space," in *Progress in Electromagnetic Research*, J. A. Kong, Ed. New York: Elsevier, 1990, vol. 4, ch. 1.
[55] F. Rachidi, "Formulation of the field-to-transmission line coupling equations in terms of magnetic excitation fields," *IEEE Trans. Electromagn. Compat.*, vol. 35, no. 3, pp. 404–407, Aug. 1993.

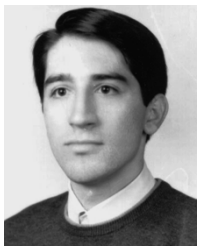

Abdolhamid Shoory was born in Khorramshahr, Iran, on April 6, 1978. He received the B.S. (with distinction) and M.S. degrees from Amirkabir University of Technology, Tehran, Iran, in 2000 and 2003, respectively, both in electrical engineering.

In 2003, he became a Research Assistant with the Electromagnetic Research Laboratory, Electrical Engineering Department, Amirkabir University of Technology. His main research interests are in the fields of numerical methods in electromagnetics, applied electromagnetics, and electromagnetic compatibility.

Mr. Shoory was the recipient of the Electrical Engineering Department Outstanding Student Award in 1999.

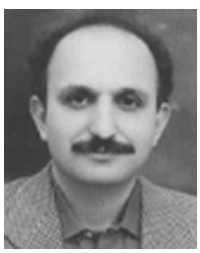

Rouzbeh Moini (A'89–M'93) was born in Tehran, Iran, in 1963. He received the B.S., M.S., and Ph.D. degrees in electronics from Limoges University, Limoges, France.

In 1988, he joined the Electrical Engineering Department, Amirkabir University of Technology, Tehran, where he is currently a Professor of telecommunications. From 1995 to 1996, he was a Visiting Professor with the University of Florida, Gainesville. His main research interests are in numerical methods in electromagnetics, electromagnetic compatibility, and antenna theory.

Dr. Moini was the recipient of the 1995 Islamic Development Bank (IDB) Merit Scholarship Award.

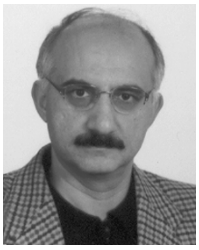

S. H. Hesam Sadeghi (M'92) received the B.S. degree in electrical engineering in 1980 from Sharif University of Technology, Tehran, Iran, the M.S. degree from the University of Manchester Institute of Science and Technology, Manchester, U.K., in 1984, and the Ph.D. degree from the University of Essex, Essex, U.K.

Between 1980 and 1983, he worked in the electrical power industry in Iran. In 1984, he became a Research Assistant with the University of Lancaster, Lancaster, U.K. He then joined the University of Essex as a Senior Research Officer. In 1992, he was appointed as a Research Assistant Professor at Vanderbilt University, Nashville, TN. From 1996 to 1997, he was a Visiting Professor with the University of Wisconsin, Milwaukee. He is presently a Professor of electrical engineering with Amirkabir University of Technology, Tehran, Iran. His current research interests include electromagnetic nondestructive testing of materials and electromagnetic compatibility problems in power engineering.

Vladimir A. Rakov (SM'96–F'03) received the M.S. and Ph.D. degrees from Tomsk Polytechnical University (Tomsk Polytechnic), Tomsk, Russia, in 1977 and 1983, respectively.

He is the author or coauthor of over 30 patents, one book, and over 300 papers and technical reports on various aspects of lightning. From 1977 to 1979, he was an Assistant Professor of electrical engineering with Tomsk Polytechnic. In 1978, he became involved in lightning research at the High Voltage Research Institute, a division of Tomsk Polytechnic, where from 1984 to 1994 he held the position of Director of the Lightning Research Laboratory. He is presently a Professor with the Department of Electrical and Computer Engineering, University of Florida, Gainesville.

Dr. Rakov is a Fellow of the American Meteorological Society. He is Chairman of the Technical Committee on Lightning of the biennial International Zurich Symposium on Electromagnetic Compatibility and former chairman of the AGU Committee on Atmospheric and Space Electricity.